Article

Molecular Cell

NF-κB-Independent Role of IKKα/IKKβ in Preventing RIPK1 Kinase-Dependent Apoptotic and Necroptotic Cell Death during TNF Signaling

Graphical Abstract

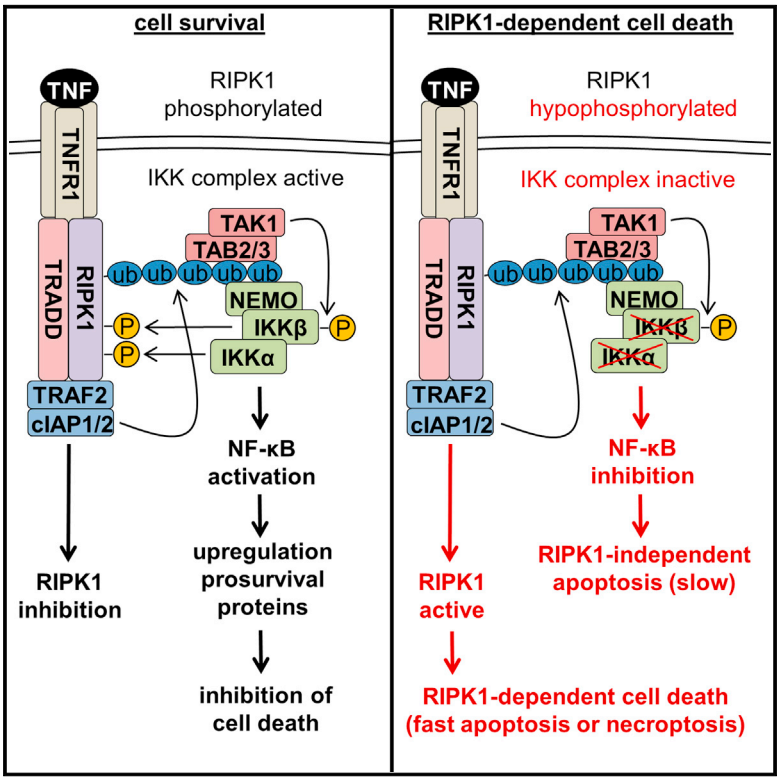

Highlights

- IKKα/IKKβ prevent RIPK1 kinase-dependent death independently of NF-κB activation
- IKKα/IKKβ directly phosphorylate RIPK1 in TNFR1 complex I
- Impaired phosphorylation of RIPK1 correlates with enhanced binding to FADD/caspase-8
- IKK kinase inhibition induces TNF-mediated RIPK1 kinase-dependent cell death in vivo

Authors

Yves Dondelinger, Sandrine Jouan-Lanhouet, Tatyana Divert, ..., Emmanuel Dejardin, Peter Vandenabeele, Mathieu J.M. Bertrand

Correspondence

mathieu.bertrand@irc.vib-ugent.be

In Brief

Dondelinger et al. describe an unexpected NF-κB-independent function of the IKK complex in protecting against TNF-induced RIPK1 kinase-dependent cell death. In TNFR1 complex I, IKKα/IKKβ directly phosphorylates RIPK1, leading to a reduction in RIPK1's ability to bind FADD/caspase-8 and to induce apoptosis.

Dondelinger et al., 2015, Molecular Cell *60*, 63–76
October 1, 2015
http://dx.doi.org/10.1016/j.molcel.2015.07.032

Molecular Cell
Article

NF-κB-Independent Role of IKKα/IKKβ in Preventing RIPK1 Kinase-Dependent Apoptotic and Necroptotic Cell Death during TNF Signaling

Yves Dondelinger,[1,2] Sandrine Jouan-Lanhouet,[1,2] Tatyana Divert,[1,2] Emilie Theatre,[3] John Bertin,[4] Peter J. Gough,[4] Piero Giansanti,[5,6] Albert J.R. Heck,[5,6] Emmanuel Dejardin,[3] Peter Vandenabeele,[1,2,7] and Mathieu J.M. Bertrand[1,2,*]
[1]Inflammation Research Center, VIB, Technologiepark 927, Zwijnaarde-Ghent 9052, Belgium
[2]Department of Biomedical Molecular Biology, Ghent University, Technologiepark 927, Zwijnaarde-Ghent 9052, Belgium
[3]Laboratory of Molecular Immunology and Signal Transduction, GIGA-Research, University of Liège, 4000 Liège, Belgium
[4]Pattern Recognition Receptor Discovery Performance Unit, Immuno-inflammation Therapeutic Area, GlaxoSmithKline, Collegeville, PA 19426, USA
[5]Biomolecular Mass Spectrometry and Proteomics, Bijvoet Centre for Biomolecular Research and Utrecht Institute for Pharmaceutical Sciences, University of Utrecht, 3584 CH Utrecht, the Netherlands
[6]Netherlands Proteomics Centre, Padualaan 8, 3584 CH Utrecht, the Netherlands
[7]Methusalem Program, Ghent University, Technologiepark 927, Zwijnaarde-Ghent 9052, Belgium
*Correspondence: mathieu.bertrand@irc.vib-ugent.be
http://dx.doi.org/10.1016/j.molcel.2015.07.032

SUMMARY

TNF is a master pro-inflammatory cytokine. Activation of TNFR1 by TNF can result in both RIPK1-independent apoptosis and RIPK1 kinase-dependent apoptosis or necroptosis. These cell death outcomes are regulated by two distinct checkpoints during TNFR1 signaling. TNF-mediated NF-κB-dependent induction of pro-survival or anti-apoptotic molecules is a well-known late checkpoint in the pathway, protecting cells from RIPK1-independent death. On the other hand, the molecular mechanism regulating the contribution of RIPK1 to cell death is far less understood. We demonstrate here that the IKK complex phosphorylates RIPK1 at TNFR1 complex I and protects cells from RIPK1 kinase-dependent death, independent of its function in NF-κB activation. We provide in vitro and in vivo evidence that inhibition of IKKα/IKKβ or its upstream activators sensitizes cells to death by inducing RIPK1 kinase-dependent apoptosis or necroptosis. We therefore report on an unexpected, NF-κB-independent role for the IKK complex in protecting cells from RIPK1-dependent death downstream of TNFR1.

INTRODUCTION

The IκB kinase (IKK) complex, composed of the regulatory subunit NEMO (also known as IKKγ) and the two catalytic subunits IKKα and IKKβ, plays a central role in the induction of immune and inflammatory responses as well as in promoting cell survival and tumorigenesis (Baldwin, 2012; Baud and Karin, 2009; Hayden and Ghosh, 2012; Liu et al., 2012). Its activation constitutes the ignition phase of the canonical NF-κB pathway, which ultimately results in the translocation of NF-κB dimers to the nucleus, where they promote transcription of a myriad of genes involved in inflammation, survival, and tumorigenesis.

TNF is a master pro-inflammatory cytokine, and inappropriate TNF signaling has been demonstrated to drive many inflammatory diseases. Activation of TNFR1 by TNF promotes inflammation either directly by activating the canonical NF-κB pathway or indirectly by promoting cell death, which exacerbates inflammation by releasing damage-associated molecular patterns (DAMPs) as well as by affecting the permeability of the bodily barriers to microbes (Pasparakis and Vandenabeele, 2015). In most cell types, activation of TNFR1 does not induce death but triggers canonical NF-κB-dependent transcriptional upregulation of genes encoding pro-survival and pro-inflammatory molecules. Ligation of TNF to trimeric TNFR1 induces the rapid assembly of a plasma membrane-bound signaling complex, known as complex I, that contains TRADD, RIPK1, and the E3 ubiquitin ligases TRAF2, cIAP1, cIAP2, and LUBAC (Walczak, 2011). The conjugation of ubiquitin chains to RIPK1 by cIAP1/cIAP2 generates binding sites for TAB2/TAB3 and NEMO and allows further recruitment and activation of TAK1 and IKKα/IKKβ (Bertrand et al., 2008; Ea et al., 2006; Gerlach et al., 2011; Kanayama et al., 2004; Mahoney et al., 2008; Wu et al., 2006). TAK1 activates the IKK complex by phosphorylation, resulting in the rapid and selective IKK-mediated phosphorylation of IκBα and in its subsequent ubiquitylation-dependent proteasomal degradation. IκBα degradation then permits translocation of the NF-κB heterodimer p50/p65 to the nucleus, where it induces transcription of multiple responsive genes, including pro-survival genes such as *cFLIP* (Hayden and Ghosh, 2014). The anti-apoptotic potential of cFLIP resides in its ability to counteract activation of caspase-8 from a cytosolic TRADD-FADD-caspase-8 cytosolic complex, named complex IIa, which is believed to originate from complex I internalization (Irmler et al., 1997; Micheau and Tschopp, 2003; Wang et al., 2008; Wilson et al., 2009). Accordingly, TNFR1-mediated RIPK1-independent apoptosis requires inhibition of the NF-κB

response (Van Antwerp et al., 1996), commonly obtained in vitro by the use of pharmacological inhibitors of transcription or translation, respectively, Actinomycin D (ActD) and cycloheximide (CHX).

The NF-κB-mediated induction of pro-survival/anti-apoptotic molecules is, however, not the only cell death checkpoint in the TNFR1 pathway (O'Donnell and Ting, 2011). Indeed, altering activation of the canonical NF-κB pathway by inhibiting components located upstream of IκBα, namely, cIAP1/cIAP2, TAK1, and NEMO, was reported to further sensitize cells to death by additionally inducing RIPK1-dependent death (Dondelinger et al., 2013; Legarda-Addison et al., 2009; O'Donnell et al., 2012). Depending on the cellular context, activated RIPK1 accelerates cell death either by promoting assembly of a RIPK1-FADD-caspase-8 cytosolic apoptotic complex, referred to as complex IIb (Wilson et al., 2009), or by promoting necroptosis via activation of the RIPK3-MLKL pathway (Pasparakis and Vandenabeele, 2015). Although initiated by cIAP1/cIAP2-mediated ubiquitylation of RIPK1 in complex I, the last molecular step in the regulation of this early RIPK1 kinase-dependent cell death checkpoint is currently unknown.

In this study, we demonstrate that RIPK1 is a bona fide substrate of IKKα and IKKβ and that IKKα/IKKβ-mediated phosphorylation of RIPK1 in complex I protects cells from RIPK1 kinase-dependent death.

RESULTS

NEMO Deficiency and IKKα/IKKβ Double Deficiencies Induce TNFR1-Mediated RIPK1 Kinase-Dependent Apoptosis

We previously reported that the ubiquitin chains conjugated to RIPK1 by cIAP1/cIAP2 do not constitute the ultimate step regulating the contribution of RIPK1 to TNF-induced cell death. Indeed, genetic or pharmacological inhibition of TAK1 also drives RIPK1-dependent death without affecting RIPK1 ubiquitylation in complex I (Dondelinger et al., 2013). In this study, we investigated the role of the IKK complex in the regulation of this cell death checkpoint. Indeed, the IKK complex lies between TAK1 and IκBα in the pathway, and although expression of a proteasome-resistant form of IκBα (IκBαSR) induces RIPK1-independent apoptosis (Dondelinger et al., 2013), NEMO deficiency was reported to sensitize cells to TNF-induced death by additionally promoting RIPK1-dependent apoptosis (Legarda-Addison et al., 2009). In absence of cIAP1/cIAP2 or TAK1, TNF-mediated RIPK1-dependent apoptosis was shown to rely on RIPK1 kinase activity (Dondelinger et al., 2013; Wang et al., 2008). To test whether this is also true in absence of NEMO, we first stimulated NEMO-deficient mouse embryonic fibroblasts (MEFs) with TNF in the absence or presence of Nec-1, a RIPK1 kinase inhibitor. Interestingly, we found that Nec-1 greatly, but not entirely, protected *Nemo*$^{-/-}$ MEFs from TNF-induced apoptosis, as monitored by cell permeability, caspase-3 activity, and caspase-3 and caspase-8 processing (Figures 1A–1D, 1K, and 1L). These results indicated that, similarly as cIAP1/cIAP2 and TAK1, NEMO also regulates both RIPK1 kinase-dependent and RIPK1-independent cell death checkpoints downstream of TNFR1. To test whether this protective function of NEMO reflects its role as adaptor protein recruiting IKKα and IKKβ to TNFR1 complex I, we next stimulated *Ikkα*$^{-/-}$, *Ikkβ*$^{-/-}$, and *Ikkα*$^{-/-}$/*Ikkβ*$^{-/-}$ MEFs with TNF. Interestingly, while IKKα or IKKβ single deficiency had little effect on apoptosis induction (Figures 1E–1H), their combined depletion mimicked the phenotype observed in the *Nemo*$^{-/-}$ MEFs (Figures 1I–1L), suggesting redundant roles of IKKα and IKKβ downstream of NEMO in preventing RIPK1-dependent apoptosis. To exclude the possibility that the phenotypes observed in the various MEF genotypes were originating from intrinsic defects due to clonal expansion, we confirmed our findings in *Ripk1*$^{+/+}$ and *Ripk1*$^{-/-}$ MEFs depleted of IKK proteins by siRNA (Figure S1). Of note, NEMO siRNA had little effect on cell death induction in these experiments, probably due to the poor efficiency in repressing NEMO.

IKKα and IKKβ Mediate Their Protective Effect on RIPK1 via Their Enzymatic Activities

Because IKKα and IKKβ are serine/threonine kinases, we next evaluated the requirement of their enzymatic activities for their ability to repress RIPK1-dependent apoptosis. To do so, we tested the effect of five different IKK inhibitors on TNF-induced death and found that all of them led to a combination of RIPK1 kinase-dependent and RIPK1-independent death, as observed in the *Ikkα*$^{-/-}$/*Ikkβ*$^{-/-}$ MEFs (Figures S2A and S2B). We further confirmed RIPK1 kinase-dependent apoptosis induction using TPCA-1 (Figures 2A–2C), as this inhibitor had no effect on TNF-induced death in *Ikkα*$^{-/-}$/*Ikkβ*$^{-/-}$ MEFs (Figure S2B). TPCA-1 was used at 5 μM, a concentration reported to inhibit both IKKα and IKKβ kinase activities (IC_{50} = 400 nM and 17.9 nM for IKKα and IKKβ, respectively) (Podolin et al., 2005). We demonstrated that the apoptotic cell death was mostly depending on RIPK1 kinase activity by either co-incubating cells with Nec-1 (Figures 2A–2C) or by stimulating RIPK1 kinase-dead-expressing MEFs (*Ripk1 K45A*) (Figures 2D and 2E) (Berger et al., 2014). Importantly, Nec-1 had no effect in *Ripk1 K45A* MEFs, excluding any off-target effect (Figures S2E andS2F). Of note, similar results were obtained upon pharmacological inhibition of cIAP1/cIAP2 or TAK1 (Figures 2F, 2G, S2C, and S2D). In line with a role of IKKα and IKKβ downstream of cIAP1/cIAP2, TAK1, and NEMO in the pathway, we tested the effect of TPCA-1 on TNF-induced death in *ciap1/2*$^{-/-}$, *Tak1*$^{-/-}$, and *Nemo*$^{-/-}$ MEFs and found no additional effect (Figures 2H–2K). Together, these results indicate that the kinase activities of IKKα/IKKβ regulate, downstream of cIAP1/cIAP2, TAK1, and NEMO, both RIPK1 kinase-dependent and RIPK1-independent cell death checkpoints.

IKKα/IKKβ Protect Cells from RIPK1-Dependent Apoptosis Independently of NF-κB

We previously demonstrated that, in absence of cIAP1/cIAP2 or TAK1, RIPK1 contribution to TNF-induced death is regulated independently of a defect in the canonical NF-κB-dependent upregulation of pro-survival genes (Dondelinger et al., 2013). Moreover, NEMO was also reported to inhibit RIPK1 activation in an NF-κB-independent manner (Legarda-Addison et al., 2009; O'Donnell et al., 2012). IKKα and IKKβ are best known for their roles in NF-κB activation, but NF-κB-independent

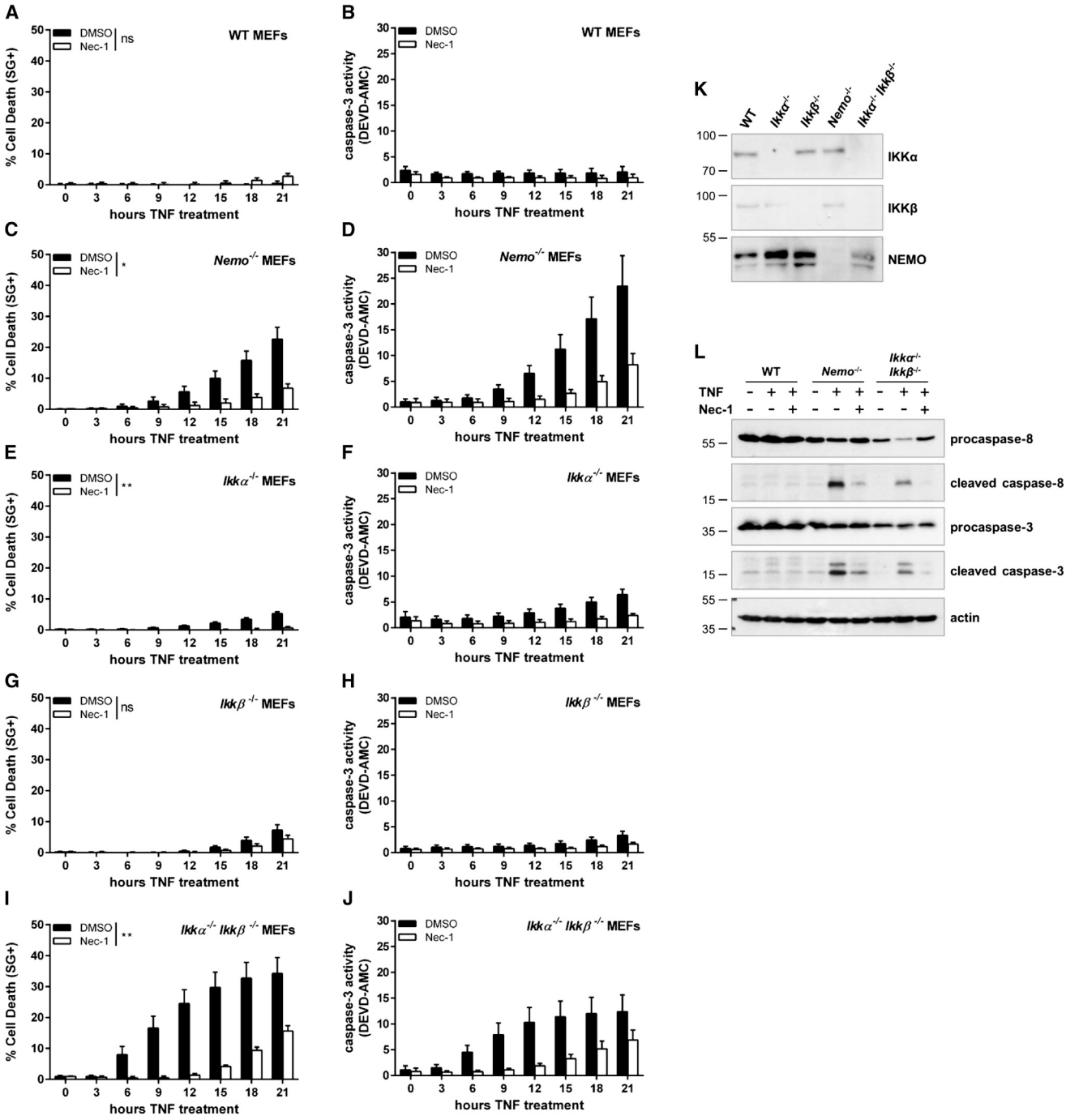

Figure 1. NEMO Deficiency and IKKα/IKKβ Double Deficiencies Induce TNFR1-Mediated RIPK1 Kinase-Dependent Apoptosis

(A–L) MEFs of the indicated genotypes were treated with 20 ng/ml hTNF in the presence or absence of Nec-1, and cell death (A, C, E, G, and I) and caspase activity (B, D, F, H, and J) were measured in function of time, respectively, by SytoxGreen positivity and DEVD-AMC fluorescence. Protein levels were determined by immunoblotting in unstimulated cells (K) or 15 hr poststimulation with the indicated compounds (L).

For the cell death results, error bars represent the SEM of three independent experiments. For the caspase-3 activity results, error bars represent SD of triplicates of one representative experiment.

See also Figure S1.

functions have also been reported (Hinz and Scheidereit, 2014). To confirm that IKKα and IKKβ regulate RIPK1 activation independently of the canonical NF-κB response, we took two different approaches. In the first one, we tested the effect of inhibiting IKKα/IKKβ in conditions where the NF-κB response is prevented by incubating the cells with the translational inhibitor

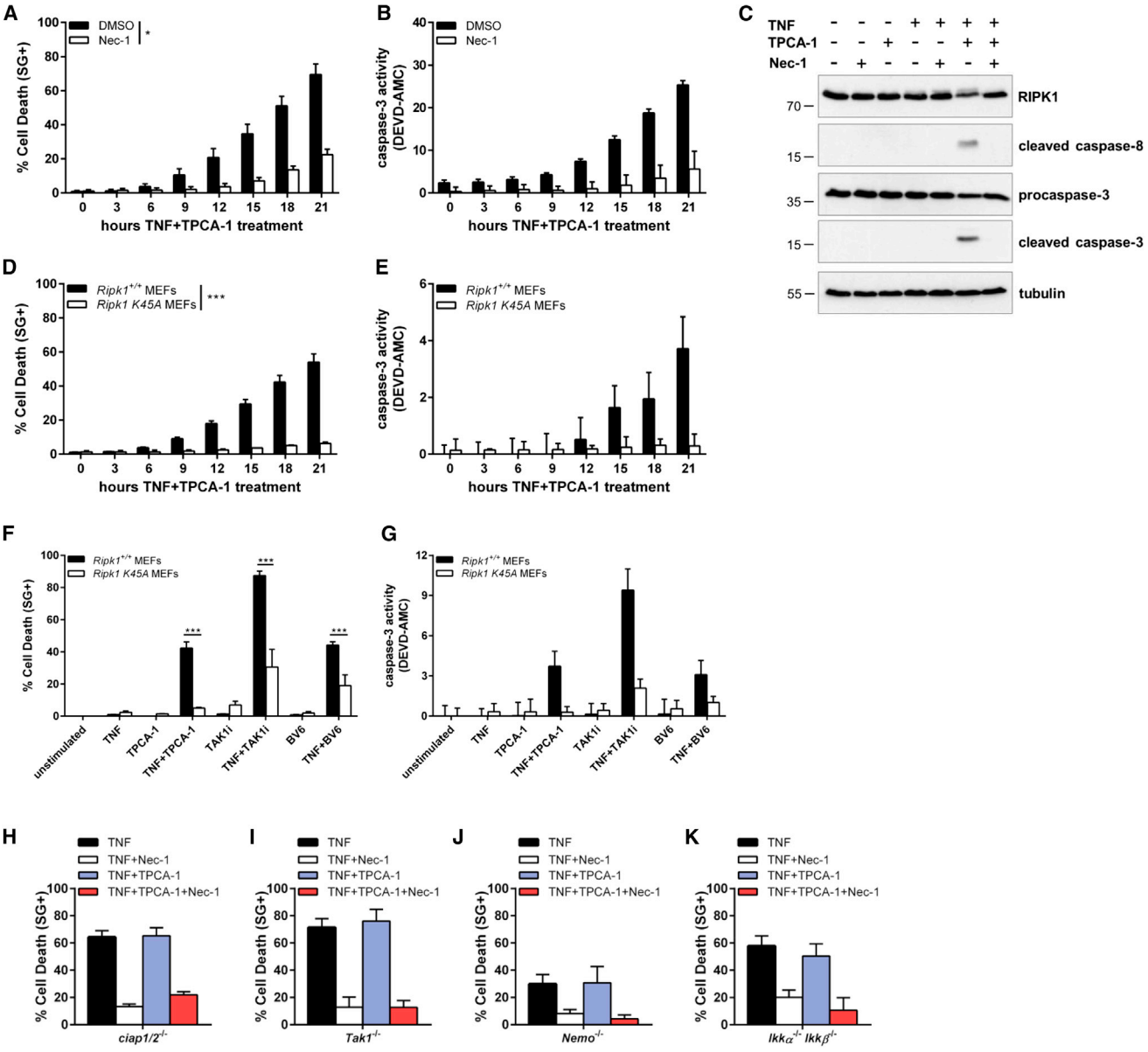

Figure 2. IKKα and IKKβ Mediate Their Protective Effect on RIPK1 via Their Enzymatic Activities

(A, B, and D–K) *Ripk1*$^{+/+}$ or MEFs of the indicated genotypes were treated with 20 ng/ml hTNF in the presence of the indicated compounds, and cell death (A, D, F, H, I, J, K) and caspase-3 activity (B, E, G) were measured in function of time, respectively, by SytoxGreen positivity and DEVD-AMC fluorescence.

(C) Protein levels in wild-type MEFs determined by immunoblotting 4 hr poststimulation.

For the cell death results, error bars represent the SEM of three independent experiments. For the caspase-3 activity results, error bars represent SD of triplicates of one representative experiment.

See also Figure S2.

CHX. In the second, we used *p65*$^{-/-}$ MEFs, which are defective for canonical NF-κB activation (Beg et al., 1995). As previously reported (Wang et al., 2008), apoptosis induced by TNF+CHX occurred with a slow kinetic and independently of RIPK1 kinase activity (Figures 3A–3C). Remarkably, a pretreatment with TPCA-1 greatly sensitized cells to apoptosis, and this sensitization was prevented by Nec-1 (Figures 3A–3C, S3A, and S3B). Similar results were obtained when stimulating NF-κB-deficient *p65*$^{-/-}$ MEFs with TNF and TPCA-1 (Figures 3D–3F) or in combination with TAK1 and cIAP1/cIAP2 inhibitors (Figures S3C and S3D). Together, these results demonstrate that RIPK1-independent and -dependent apoptotic pathways are regulated by two different cell death checkpoints downstream of TNFR1 and that IKKα/IKKβ regulate both of them in NF-κB-dependent and -independent manners, respectively.

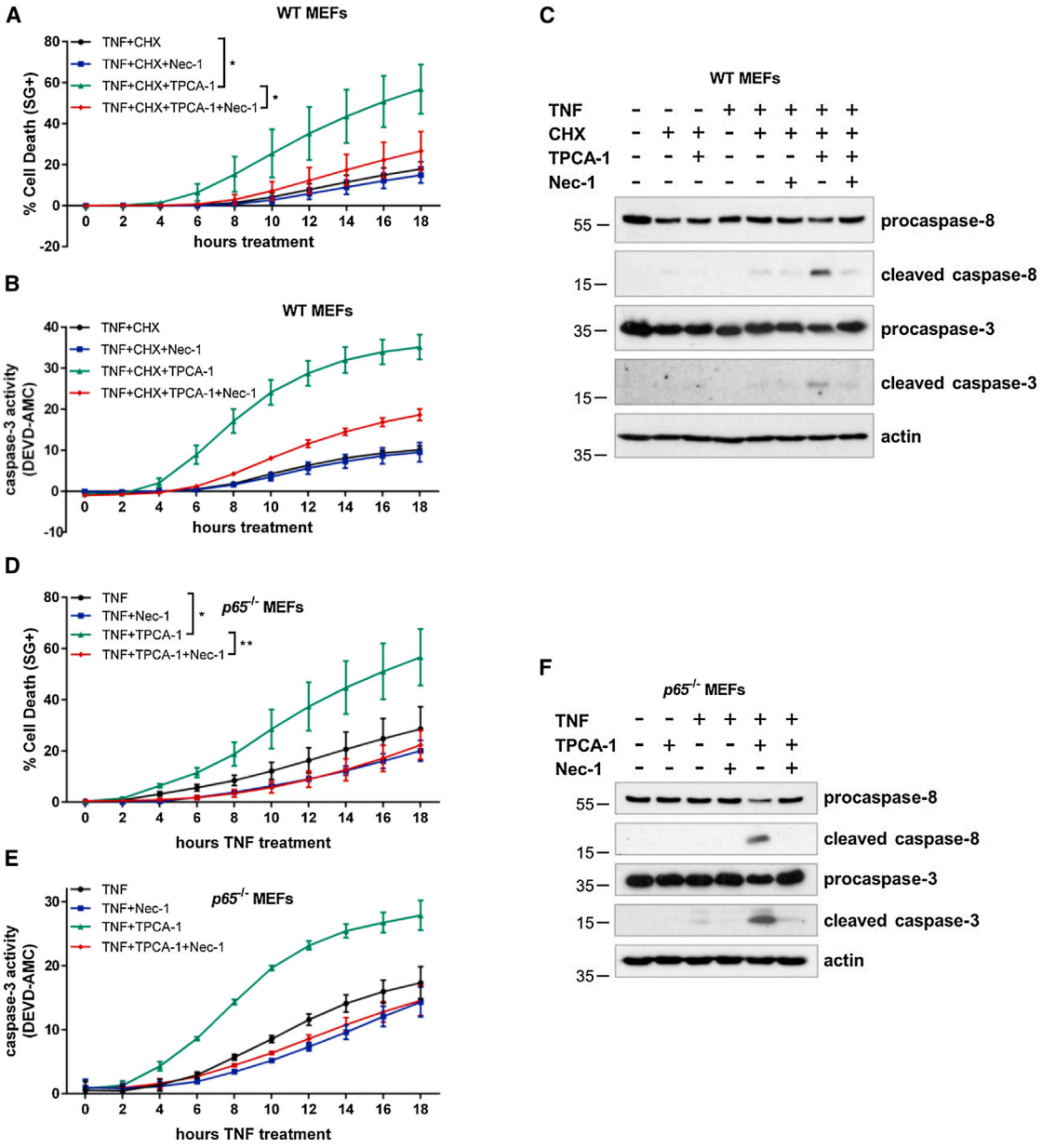

Figure 3. IKKα/IKKβ Protect Cells from RIPK1-Dependent Apoptosis Independently of NF-κB

(A, B, D, and E) *Ripk1*$^{+/+}$ (A and B) or *p65*$^{-/-}$ (D and E) MEFs were stimulated with 20 ng/ml hTNF in the presence of the indicated compounds, and cell death (A and D) and caspase activity (B and E) were measured in function of time, respectively, by SytoxGreen positivity and DEVD-AMC fluorescence.

(C and F) *Ripk1*$^{+/+}$ (C) or *p65*$^{-/-}$ (F) MEFs were stimulated for, respectively, 15 hr and 8 hr with the indicated compounds, and protein levels were determined by immunoblotting.

For the cell death results, error bars represent the SEM of three independent experiments. For the caspase-3 activity results, error bars represent SD of triplicates of one representative experiment.

See also Figure S3.

Defective RIPK1 Phosphorylation in Complex I Correlates with RIPK1 Kinase-Dependent Contribution to TNF-Induced Apoptosis

Knowing that the IKK complex physically interacts with RIPK1 in complex I, we hypothesized that the kinase-dependent role of IKKα/IKKβ in preventing RIPK1 kinase-dependent apoptosis results from its ability to phosphorylate RIPK1. To test this hypothesis, we analyzed whether RIPK1 is phosphorylated in complex I and whether its phosphorylation state is altered in conditions affecting activation of IKKα/IKKβ, but not when the pathway is inhibited downstream of IKKα/IKKβ. Because RIPK1 is highly ubiquitylated in complex I (which prevents the detection by immunoblot of potential mobility shifts resulting from its phosphorylation), we removed the ubiquitin chains conjugated to

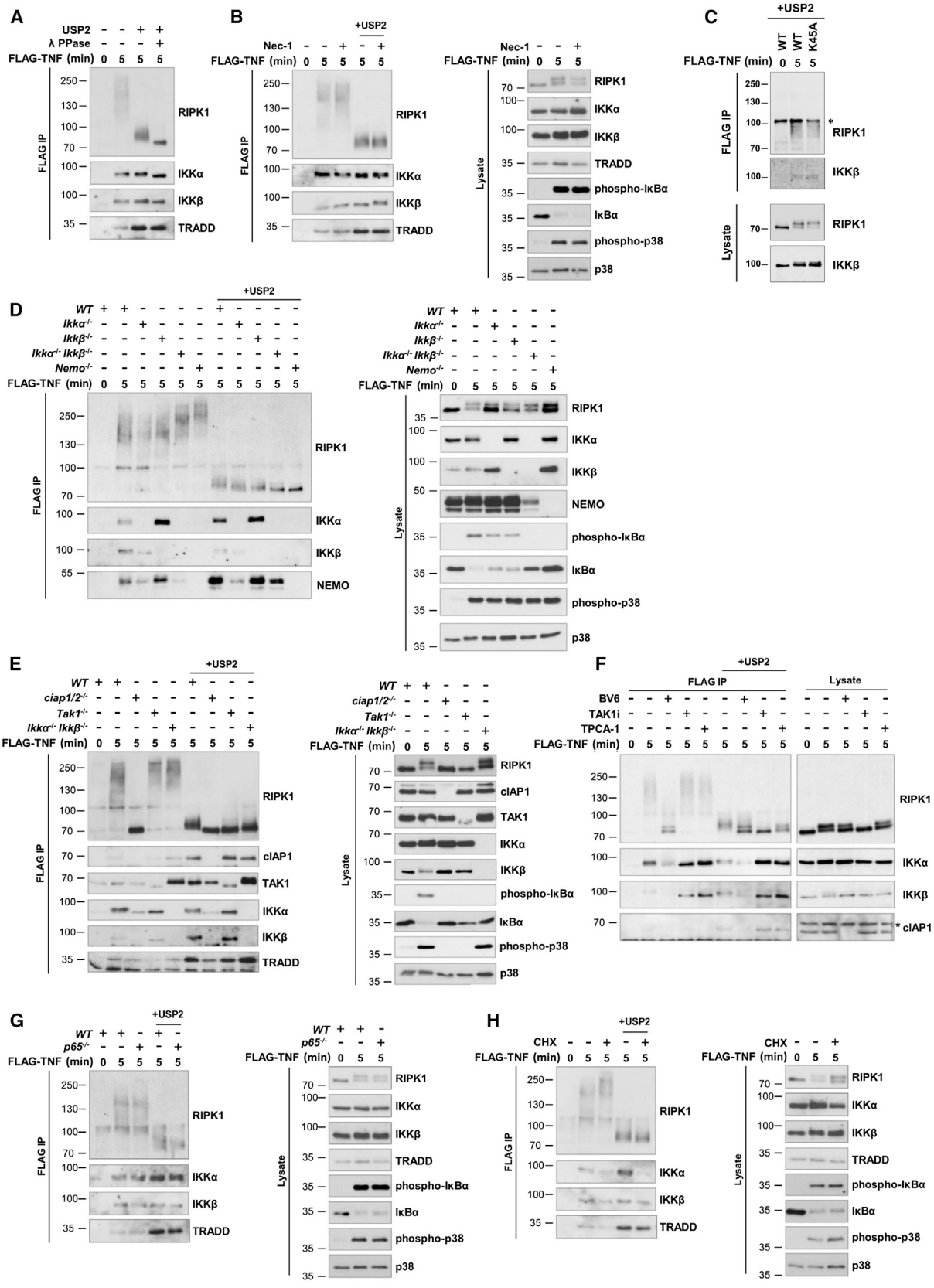

(legend on next page)

RIPK1 by incubating complex I, pulled-down using FLAG-TNF, with the deubiquitylase USP2 (Figure 4A). By doing so, we observed that the pool of deubiquitylated RIPK1 was running at a higher molecular weight than normal and confirmed, by λ-phosphatase treatment, that this mobility shift was resulting from phosphorylation, but not auto-phosphorylation since it was not inhibited by Nec-1 or in *Ripk1 K45A* MEFs (Figures 4A–4C). Remarkably, and in line with the model of cIAP1/cIAP2-mediated ubiquitylation-dependent recruitment of TAK1 and NEMO/IKKα/IKKβ to complex I and with our cell death results, we found that RIPK1 phosphorylation in complex I is affected in *ciap1/2*$^{-/-}$, *Tak1*$^{-/-}$, *Nemo*$^{-/-}$, and *Ikkα*$^{-/-}$/*Ikkβ*$^{-/-}$, but not in *Ikkα*$^{-/-}$, *Ikkβ*$^{-/-}$, and *p65*$^{-/-}$ MEFs or in MEFs pre-incubated with CHX (Figures 4D, 4E, 4G, and 4H). Importantly, IKK activity is greatly affected (as observed by IκBα phosphorylation) in all conditions in which we observed impaired RIPK1 phosphorylation, thereby further demonstrating the link between RIPK1 phosphorylation and IKK enzymatic activities (Figure 4E). Defective RIPK1 phosphorylation in complex I was also observed following pharmacological inhibition of cIAP1/cIAP2, TAK1, or IKKα/IKKβ (Figure 4F).

Direct Phosphorylation of RIPK1 by IKKα/IKKβ Prevents RIPK1 from Integrating Complex IIb

To test the direct contribution of IKKα/IKKβ to RIPK1 phosphorylation, we next performed in vitro kinase assays using recombinant proteins and included Nec-1 in the reactions to prevent RIPK1 autophosphorylation. We found that both IKKα and IKKβ directly phosphorylated full-length RIPK1 or a mutated version lacking the death and RHIM domain (RIPK1$^{1-479}$) (Figures 5A, 5B, and S4A). Of note, RIPK1 phosphorylation by IKKβ induced a mobility shift of RIPK1 not detected when using IKKα (Figures 5A and 5B), suggesting some specificity in the residues phosphorylated by both kinases. In line with our cellular data, TPCA-1 repressed, although with different efficiencies, the direct phosphorylation of RIPK1 by IKKα and IKKβ. In contrast, recombinant TAB1/TAK1 did not lead to detectable RIPK1 phosphorylation by autoradiography (Figure 5C).

We next tested the consequence of genetic or pharmacological inhibition of IKKα/IKKβ, and of the resulting defective phosphorylation of RIPK1 in complex I, on the ability of RIPK1 to integrate the cytosolic caspase-8-activating complex IIb. We found, by performing FADD and caspase-8 immunoprecipitations, that inhibition of IKKα/IKKβ enzymatic activities resulted in the binding of RIPK1 to FADD and caspase-8, a process relying on RIPK1 kinase activity (Figures 5D–5G). In contrast, CHX pre-treatment, which does not affect phosphorylation of RIPK1 in complex I (Figure 4H), led to much less recruitment of RIPK1 to FADD/caspase-8, and this recruitment was not inhibited by Nec-1 (Figures 5F, 5G, and S4B). Of note, association of TRADD with FADD/caspase-8 was not observed under these conditions. Together, these results suggest that IKKα/IKKβ-mediated phosphorylation of RIPK1 either represses RIPK1 kinase activity or interferes with RIPK1's ability to bind complex IIb components.

IKKα/IKKβ Mediate In Vivo Protection to RIPK1 Kinase-Dependent Death

To test the in vivo relevance of our in vitro findings, we evaluated the contribution of RIPK1 kinase activity to two different mouse models of TNF-induced death. In the first one, we injected *Ripk1*$^{K45A/K45A}$ and *Ripk1*$^{+/+}$ littermates with TNF in association with D-galactosamine. In this well-known model of acute hepatitis, TNF-mediated hepatocyte apoptosis is reported to result from transcriptional inhibition (Decker and Keppler, 1974), thereby affecting the NF-κB pathway downstream of IKKα/IKKβ. In accordance with our in vitro results, we found that *Ripk1*$^{K45A/K45A}$ mice were not protected from TNF-induced lethality and apoptotic liver damage, as monitored by survival curves, blood levels of aspartate transaminase/alanine transaminase (AST/ALT), caspase-3 activation in the liver by DEVDase assays, and active caspase-3 staining (Figures 6A–6E). Blood levels of lactate dehydrogenase (LDH), a marker of necrosis, were not upregulated by TNF+GalN injection (Figure 6F).

In the next model, we injected *Ripk1*$^{K45A/K45A}$ and *Ripk1*$^{+/+}$ littermates with a sub-lethal dose of TNF (5 μg) in presence or absence of TPCA-1 (10 mg/kg) to inhibit the canonical NF-κB pathway at the level of IKKα/IKKβ. Remarkably, while TPCA-1 had no toxicity on its own (Figures S5A and S5B), its combination with TNF resulted in the rapid death of all *Ripk1*$^{+/+}$, but no *Ripk1*$^{K45A/K45A}$, mice (Figure 6G). Accordingly, *Ripk1*$^{K45A/K45A}$ mice were protected from TNF-induced hypothermia and had no increase in serum levels of ASL/ALT or caspase-3 activation in the liver (Figures 6H–6L). In contrast to TNF+GalN injection, TNF+TPCA-1 led to a substantial increase of LDH levels in the serum that was also absent in *Ripk1*$^{K45A/K45A}$ mice, suggesting additional necroptosis induction (Figure 6M). Importantly, RIPK1 kinase inhibition by co-administration of Nec-1s (Degterev et al., 2013), a modified and more stable version of Nec-1, in C57BL/6J mice also significantly delayed the death and injury induced by TNF+TPCA-1 injection (Figures S5C–S5I).

Together, these in vivo results demonstrate TNF-mediated RIPK1-independent and RIPK1 kinase-dependent hepatocyte apoptosis in condition of NF-κB inhibition downstream or at the level of IKKα/IKKβ, respectively.

IKKα/IKKβ Protect Cells from RIPK1 Kinase-Dependent Necroptosis Independently of NF-κB

Our in vivo results suggested that TNF+TPCA-1 additionally induced necroptosis in the injected mice. To test the possibility that IKKα/IKKβ also regulates RIPK1 kinase-dependent necroptosis independently of NF-κB, we in vitro stimulated MEFs with TNF+CHX in the presence of the pan caspase inhibitor zVAD-fmk and of TPCA-1. As shown in Figure 7A, TNF-mediated

Figure 4. Defective RIPK1 Phosphorylation in Complex I Correlates with RIPK1 Kinase-Dependent Contribution to TNF-Induced Apoptosis

(A–H) *Ripk1*$^{+/+}$ MEFs (A, B, F, and H) or MEFs with the indicated genotype (C, D, E, and G) were stimulated for 5 min with 2 μg/ml FLAG-hTNF in the presence or absence of the indicated compounds. TNFR1 complex I was then FLAG immunoprecipitated, incubated with the deubiquitylating enzyme USP2 or lambda phosphatase (λ PPase) when indicated, and RIPK1 ubiquitylation and phosphorylation finally analyzed by immunoblotting. * indicates an aspecific band.
See also Figure S7.

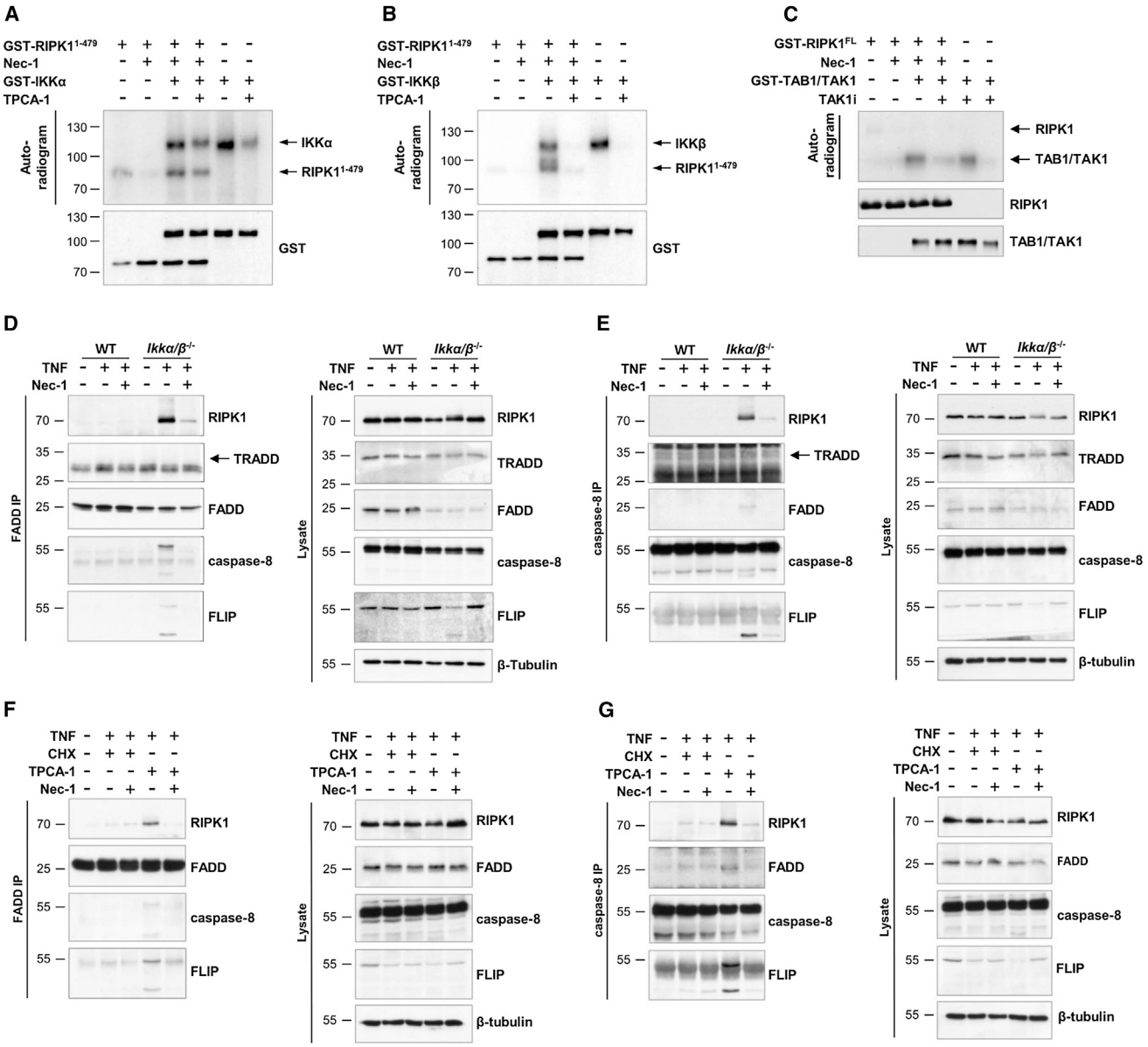

Figure 5. Direct Phosphorylation of RIPK1 by IKKα/IKKβ Prevents RIPK1 from Integrating Complex IIb

(A–C) Recombinant GST-IKKα, GST-IKKβ, or GST-TAB1-TAK1 fusion protein was incubated with a recombinant truncated (GST-RIPK1$^{1–479}$) or full-length (GST-RIPK1^{FL}) form of RIPK1 in a radioactive in vitro kinase assay in the presence of the indicated inhibitors. Phosphorylation was revealed by SDS-PAGE followed by autoradiography.

(D–G) MEFs with the indicated genotype (D and E) or *Ripk1*$^{+/+}$ MEFs (F and G) were pre-incubated with zVAD-fmk and with the indicated compounds for 30 min and then stimulated with 20 ng/ml hTNF. After 4 hr, complex II was isolated by FADD or caspase-8 immunoprecipitation and RIPK1 binding revealed by immunoblotting.

See also Figure S4.

necroptosis induced by TNF+CHX+zVAD is fully repressed by Nec-1 but still greatly enhanced by additionally inhibiting IKKα/IKKβ with TPCA-1 (Figures 7A and S6A). The mouse fibrosarcoma cell line L929sAhFAS is a prototypic model for necroptosis since these cells succumb by necroptosis upon single TNF stimulation. While inhibiting NF-κB by CHX sensitized these cells to necroptosis, the sensitization was again enhanced when IKKα/IKKβ was additionally inhibited by TPCA-1 (Figures 7B and S6B). Our results therefore demonstrate that IKKα/IKKβ prevent RIPK1 kinase-dependent apoptosis and necroptosis downstream of TNFR1 independently of their known function in protecting the cells from death by mediating NF-κB-dependent upregulation of pro-survival/anti-death genes.

RIPK1 kinase-dependent necroptosis relies on the downstream activation of the RIPK3-MLKL pathway (Cho et al., 2009; He et al., 2009; Pasparakis and Vandenabeele, 2015;

Sun et al., 2012; Zhang et al., 2009; Zhao et al., 2012). To further characterize the contribution of RIPK3 to the lethality resulting from the in vivo injection of TNF+TPCA-1, we challenged *Ripk3*$^{+/+}$ and *Ripk3*$^{-/-}$ littermates with this trigger. Contrary to *Ripk1*$^{K45A/K45A}$ mice, *Ripk3*$^{-/-}$ mice were greatly, but not entirely, protected from death and hypothermia induced by TNF+TPCA-1 (Figures 7C and 7D). Interestingly, the protection was not originating from the liver, as RIPK3 deficiency did not prevent liver damage (Figures 7E–7H). Instead, RIPK3 deficiency prevented the increased of LDH levels in the blood, resulting from necrosis of undefined organ(s) (Figure 7I). These in vivo results therefore suggest that the lethality induced by TNF+TPCA-1 results from both RIPK1 kinase-dependent apoptosis and necroptosis.

DISCUSSION

Sensing of TNF by TNFR1 at the cell surface can paradoxically result in the activation of signaling pathways with opposite consequences: cell survival or cell death. The fact that survival is the dominant outcome in most cell types indicates the existence of molecular mechanisms actively repressing TNFR1-mediated cell death. Two major mechanisms have been reported to control cell death downstream of TNFR1 (O'Donnell and Ting, 2011). The first identified one is well characterized and consists in a relatively slow process involving the NF-κB-dependent induction of pro-survival/anti-death molecules, such as cFLIP (Karin and Lin, 2002; Kreuz et al., 2001; Liu et al., 1996; Micheau et al., 2001; Panayotova-Dimitrova et al., 2013; Van Antwerp et al., 1996; Wang et al., 1998). The second one, which is less understood and more recently reported, is believed to take place at an earlier stage following TNFR1 activation and is shown to be independent of the NF-κB response (Dondelinger et al., 2013; Legarda-Addison et al., 2009; O'Donnell et al., 2007, 2012; Wang et al., 2008). Interestingly, while the first checkpoint regulates slow apoptosis by inhibiting activation of complex IIa (TRADD-FADD-caspase-8), the second one regulates the contribution of RIPK1 to cell death by either preventing RIPK1 from integrating the apoptotic complex IIb (RIPK1-FADD-casapase-8) or by limiting its contribution to the necrosome (RIPK1-RIPK3-MLKL) (Cho et al., 2009; He et al., 2009; Sun et al., 2012; Vanlangenakker et al., 2011; Wang et al., 2008; Wilson et al., 2009; Zhang et al., 2009; Zhao et al., 2012). It has long been thought that IKKα/IKKβ inhibits TNF-induced cell death through activation of the NF-κB pathway. In this study, we provide evidences that IKKα and IKKβ also regulate cell death by direct phosphorylation of RIPK1 at the level of TNFR1 complex I.

TNF-induced RIPK1-dependent apoptosis was first described in conditions affecting cIAP1/cIAP2-mediated RIPK1 ubiquitylation (Bertrand et al., 2008; O'Donnell et al., 2007; Petersen et al., 2007; Wang et al., 2008), which led to the hypothesis that the ubiquitin chains on RIPK1 were directly preventing its binding to FADD, keeping RIPK1 in a survival modus. This "direct" effect, however, has later been challenged. Binding of the adaptor proteins TABs and NEMO to RIPK1 ubiquitin chains allows recruitment of TAK1 and of IKKα/IKKβ to TNFR1 complex I (Ea et al., 2006; Li et al., 2006; Wu et al., 2006), and TAK1 inhibition was shown to result in TNF-mediated RIPK1-dependent apoptosis without affecting RIPK1 ubiquitylation status (Dondelinger et al., 2013). We show here that RIPK1 is phosphorylated in complex I and that affecting RIPK1 ubiquitylation by cIAP1/cIAP2 depletion directly impacts its phosphorylation. In contrast, TAK1, NEMO, or IKKα/IKKβ depletion affects RIPK1 phosphorylation and induces RIPK1-dependent cell death but does not alter its ubiquitylation state in complex I. Together, these results indicate that ubiquitylation and phosphorylation of RIPK1 occur sequentially and that RIPK1 phosphorylation regulates its killing potential. Because activation of the IKK complex lies downstream of TAK1 but upstream of IκBα and p65, our results suggest a model in which IKKα/IKKβ constitute the last step in the regulation of the RIPK1 cell death checkpoint (graphical abstract). Indeed, p65 deletion, expression of IκBαSR, or CHX pre-treatment induces TNF-mediated RIPK1-independent apoptosis and does not alter RIPK1 ubiquitylation or phosphorylation in complex I.

RIPK1 enzymatic activity is needed for the integration of RIPK1 to complex IIb and to the necrosome, which respectively drives apoptosis or necroptosis under TNF-stimulated conditions (Cho et al., 2009; Dondelinger et al., 2013; He et al., 2009; Wang et al., 2008). The precise role of RIPK1 kinase activity in these processes remains unclear but may involve autophosphorylation-driven conformational changes allowing increased binding of RIPK1 to the death complex components. The kinase activity of RIPK1 therefore requires active repression to avoid unnecessary cell death. A recent report suggests that RIPK1 phosphorylation on Ser89 suppresses its kinase activity (McQuade et al., 2013). It is therefore tempting to speculate that IKK-mediated phosphorylation of RIPK1 in complex I affects RIPK1 kinase activity. Alternatively, the phosphorylation of RIPK1 by IKKs may directly affect binding of RIPK1 to the death complex components or facilitate its dissociation from complex I. We performed mass spectrometry analysis to identify the residues of RIPK1 phosphorylated by IKKα and IKKβ and found several sites, but not Ser89 (Figures S4C and S4D). Unfortunately, we were unable to demonstrate the direct physiological relevance of the identified phosphorylation sites due to the fact that all *Ripk1*$^{-/-}$ reconstituted MEFs, even those with WT RIPK1 (irrespective of RIPK1 expression levels), started to succumb upon single TNF stimulation (data not shown), a problem previously reported (Gentle et al., 2011). The fact that the combined repression of IKKα and IKKβ is needed to induce RIPK1 kinase-dependent death, and that the phosphorylation by each kinase results in different RIPK1 mobility shifts when run on gels, may indicate that phosphorylation on several residues is required to negatively regulate RIPK1.

IKKα and IKKβ are best known for their roles in NF-κB activation, but NF-κB-independent functions have also been reported, some of which are even implicated in cell fate decisions (Hinz and Scheidereit, 2014). Using pharmacological inhibition of IKKα/IKKβ in a p65-deficient background, or together with CHX, we demonstrated an NF-κB-independent function of IKKα/IKKβ in protecting cells from TNF-induced RIPK1 kinase-dependent apoptosis and necroptosis. In vivo, we demonstrate that TNF induces apoptosis of hepatocytes independently of RIPK1 when the NF-κB pathway is affected downstream of IKKα/IKKβ (TNF+GalN). In contrast, pharmacological inhibition of the NF-κB pathway at the level of IKKα/IKKβ (TNF+TPCA-1)

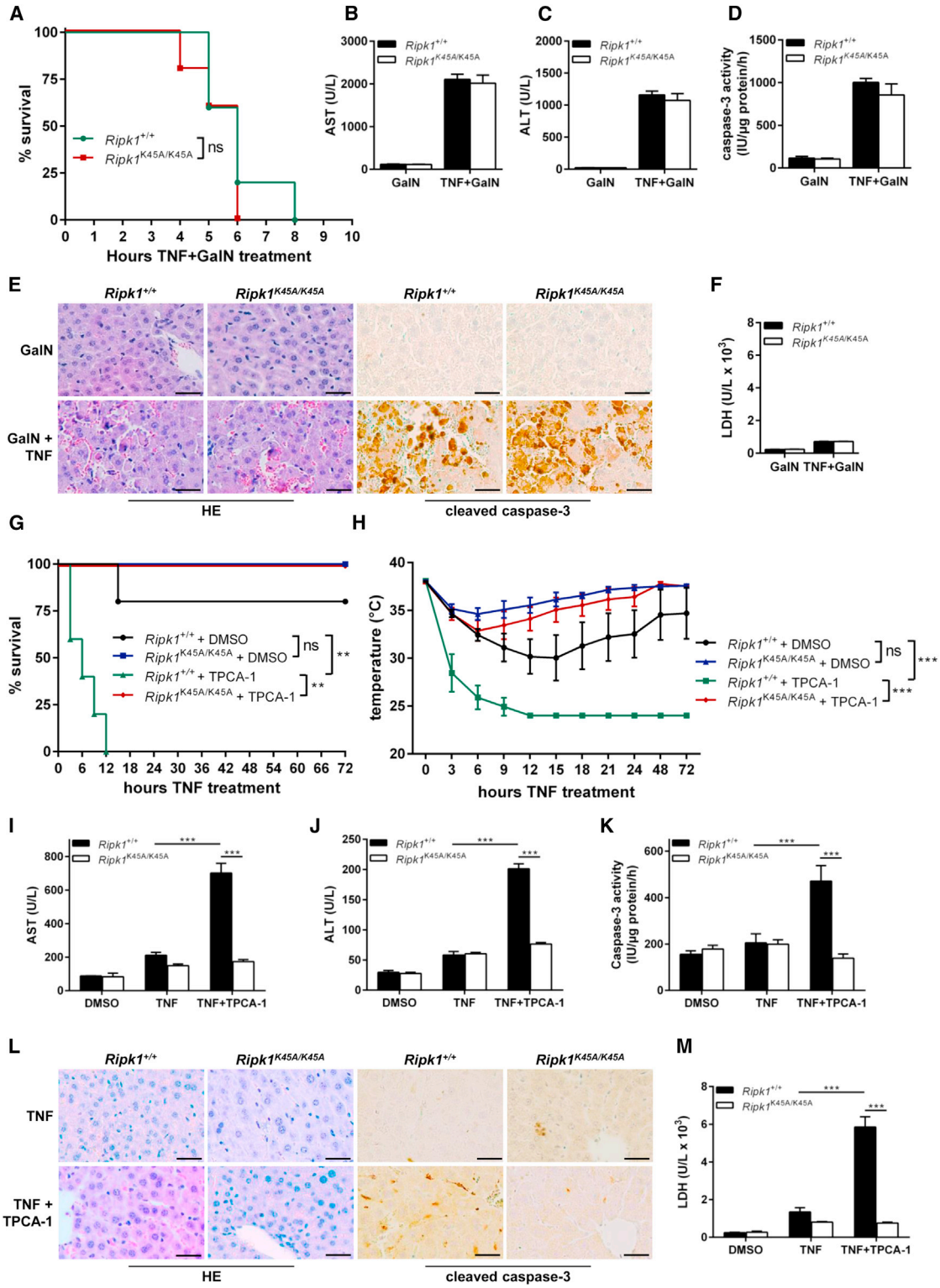

Figure 6. IKKα/IKKβ Mediate In Vivo Protection to RIPK1 Kinase-Dependent Death

(A) Cumulative survival rates of littermate *Ripk1*$^{+/+}$ and *Ripk1*$^{K45A/K45A}$ C57BL/6J females injected with GalN 15 min prior to injection with mTNF (n = 5).

(B, C, and F) Blood AST (B), ALT (C), and LDH (F) levels determined 3 hr post-TNF injection (*Ripk1*$^{+/+}$ n = 3, and *Ripk1*$^{K45A/K45A}$ n = 4).

(D and E) Caspase-3 activity in liver samples (*Ripk1*$^{+/+}$ n = 3, and *Ripk1*$^{K45A/K45A}$ n = 4) isolated 3 hr post-TNF injection and determined by Ac-DEVD-AMC fluorescence assay (D) or anti-cleaved caspase-3 staining (E).

(legend continued on next page)

sensitizes mice to TNF-induced shock, which is accompanied by RIPK1 kinase-dependent, but RIPK3-independent, apoptosis of hepatocytes and RIPK1/RIPK3-dependent cellular death, presumably necroptosis, in undefined organs. We can indeed not formally rule out the possibility that the increase in serum LDH levels originates from secondary necrosis of apoptotic cells. Importantly, genetic and chemical inhibition of RIPK1 enzymatic activity protected the mice from TNF-induced cellular damage and death. These results therefore demonstrate the in vivo roles of IKKα/IKKβ in protecting cells from RIPK1 kinase-dependent death.

The LUBAC complex, which includes its component Sharpin, is recruited to complex I during TNF signaling, and the inactivating mouse *Sharpin cpdm* mutation was reported to cause multi-organ inflammation resulting from TNF-mediated RIPK1 kinase-dependent death (Berger et al., 2014; Kumari et al., 2014; Rickard et al., 2014). In line with our results, we found that TNF-mediated RIPK1 kinase-dependent death of mouse dermal fibroblasts (MDFs) isolated from *Sharpin*^{cpdm} mice is associated with defective RIPK1 phosphorylation in complex I (Figures S7A and S7B), probably resulting from the altered recruitment of IKK proteins to complex I, as previously reported for other LUBAC components (Haas et al., 2009).

The genetic disruption of *Nemo*, *Ikkα*, *Ikkβ*, or *Ikkα*/*Ikkβ* in mice results in early lethality with massive cellular death in several organs, such as the liver, the skin, and, in the case of *Ikkα*$^{-/-}$/β$^{-/-}$ mice, the nervous system (Hu et al., 1999; Li et al., 1999, 2000; Rudolph et al., 2000; Takeda et al., 1999). So far, these phenotypes have exclusively been explained by defects in NF-κB activation, but our study indicates that RIPK1 activation probably contributes to these pathological conditions. In the same line, RIPK1 kinase-dependent apoptosis may drive the spontaneous development of hepatocellular carcinoma observed in mice ablated of *Nemo* in the liver parenchymal cells (Luedde et al., 2007). Testing the contribution of RIPK1 to those phenotypes is an exciting future challenge, which may open doors for the use of chemical inhibitors of RIPK1 in the treatment of human diseases associated with IKK malfunctions, such as incontinentia pigmenti (Conte et al., 2014).

EXPERIMENTAL PROCEDURES

Antibodies and Reagents

All antibodies and reagents used in this study are listed in the Supplemental Experimental Procedures.

Cell Lines

MEFs and L929sAhFas were cultured in DMEM supplemented with 10% fetal calf serum, L-glutamine (200 mM), and sodium pyruvate (400 mM). Primary *Ripk1*$^{+/+}$ and *Ripk1 K45A* MEFs were isolated from E12.5 littermate embryos following standard protocol and cultured under low-oxygen conditions (3% O_2). Immortalized *Ripk1*$^{-/-}$, *ciap1/2*$^{-/-}$, *Tak1*$^{-/-}$, *Ikkα*$^{-/-}$, *Ikkβ*$^{-/-}$, *Nemo*$^{-/-}$, *Ikkα*$^{-/-}$*Ikkb*$^{-/-}$, and *p65*$^{-/-}$ MEFs have previously been reported (Dejardin et al., 2002; Dondelinger et al., 2013; Moulin et al., 2012) and were cultured in normoxic conditions. Experiments were performed with MEFs derived from single animals.

Analysis of Cell Death and Caspase-3 Activation

MEFs were seeded day before at 10,000 cells per well in duplicates in a 96-well plate. The next day, cells were pre-treated with the indicated compounds for 30 min and then stimulated with hTNF (20 ng/ml–600 IU/ml) in the presence of 5 μM SytoxGreen (Invitrogen) and 20 μM Ac-DEVD-MCA (PeptaNova). SytoxGreen intensity and caspase-3 activation were measured at intervals of 1 hr using a Fluostar Omega fluorescence plate reader, with an excitation filter of 485 nm (SytoxGreen) or 360 nm (Ac-DEVD-MCA), emission filter of 520 nm (SytoxGreen) or 460 nm (Ac-DEVD-MCA), gains set at 1,100, 20 flashes per well, and orbital averaging with a diameter of 3 mm. Percentage of cell death was calculated as (induced fluorescence − background fluorescence)/(max fluorescence − background fluorescence)*100. The maximal fluorescence is obtained by full permeabilization of the cells using Triton X-100 at a final concentration of 0.1%.

Immunoprecipitation

For complex I immunoprecipitations (IPs), 5.10^6 MEF cells were seeded the day before in a 145 cm^2 tissue culture plate. After 30 min of pre-treatment, the MEF cells were stimulated with 2 μg/ml FLAG-hTNF. Cells were washed two times in ice-cold PBS before lysis in 1 ml of NP-40 lysis buffer (10% glycerol, 1% NP-40, 150 mM NaCl, and 10 mM Tris-HCl [pH 8] supplemented with phosphatase and protease inhibitor cocktail tablets [Roche Diagnostics]). The cell lysates were cleared by centrifugation for 15 min at 4°C, and the supernatant was then incubated overnight with FLAG M2 affinity gel. The next day, the beads were washed three times in NP-40 lysis buffer. The beads were then either resuspended in 1× Laemmli buffer to elute the immune complexes or resuspended in 1× DUB/λPP buffer (50 mM Tris-HCl [pH 8], 50 mM NaCl, 5 mM DTT, and 1 mM $MnCl_2$) to remove conjugated ubiquitin chains and phosphorylations on RIPK1. Then, either 1.8 μg USP2 or 800 U Lambda protein phosphatase (New England BioLabs) was added as indicated. Reactions were incubated for 30 min at 30°C and subsequently 30 min at 37°C.

For complex II IPs, 2.10^6 MEF cells were seeded the day before in a 60 cm^2 culture plate. After 30 min of pre-treatment with zVAD-fmk, MEF cells were stimulated with 20 ng/ml hTNF for the indicated time. Then, cells were washed two times in ice-cold PBS before lysis in 1 ml of NP-40 lysis buffer. The cell lysates were cleared by centrifugation for 15 min at 4°C, and the supernatant was then incubated overnight with protein A Sepharose CL-4B (GE Healthcare) and 3 μL homemade polyclonal rabbit anti-mouse caspase-8 or 10 μL of anti-FADD (M-19) (Santa Cruz Biotechnology #sc-6036) antibodies. The next day, the beads were washed three times in NP-40 lysis buffer. The immune complexes were then eluted in 2× Laemmli buffer and analyzed by western blotting.

In Vitro Kinase Assays

Kinase assays were performed for 30 min at 30°C with 250 ng of the indicated recombinant protein(s) in 30 μL of kinase buffer (20 mM HEPES [pH 7.5], 10 mM $MgCl_2$, 2 mM DTT, phosphatase inhibitor cocktail, and EDTA-free protease inhibitor, 10 μM ATP, and 10 μCi ATP γ-P^{32}). Kinase reactions were quenched by addition of 5× Laemmli buffer and by boiling the samples for 5 min.

Mice Injections, Monitoring, and Sampling

A detailed description of the protocols used for the in vivo experiments and for the processing of the samples is provided in the Supplemental Experimental Procedures. All experiments on mice were conducted according to institutional, national, and European animal regulations.

(G) Cumulative survival rates of littermate *Ripk1*$^{+/+}$ and *Ripk1*$^{K45A/K45A}$ C57BL/6J females injected with TPCA-1 20 min prior to injection with mTNF (n = 5).
(H) Body temperature as a function of time.
(I, J, and M) Blood AST (I), ALT (J), and LDH (M) levels determined 3 hr post-TNF injection (n = 4).
(K and L) Caspase-3 activity in liver samples (n = 4) isolated 3 hr post-TNF injection and determined by Ac-DEVD-AMC fluorescence assay (K) or anti-cleaved caspase-3 staining (L).
Scale bar, 25 μm. Error bars represent the SEM of the indicated n values.
See also Figure S5.

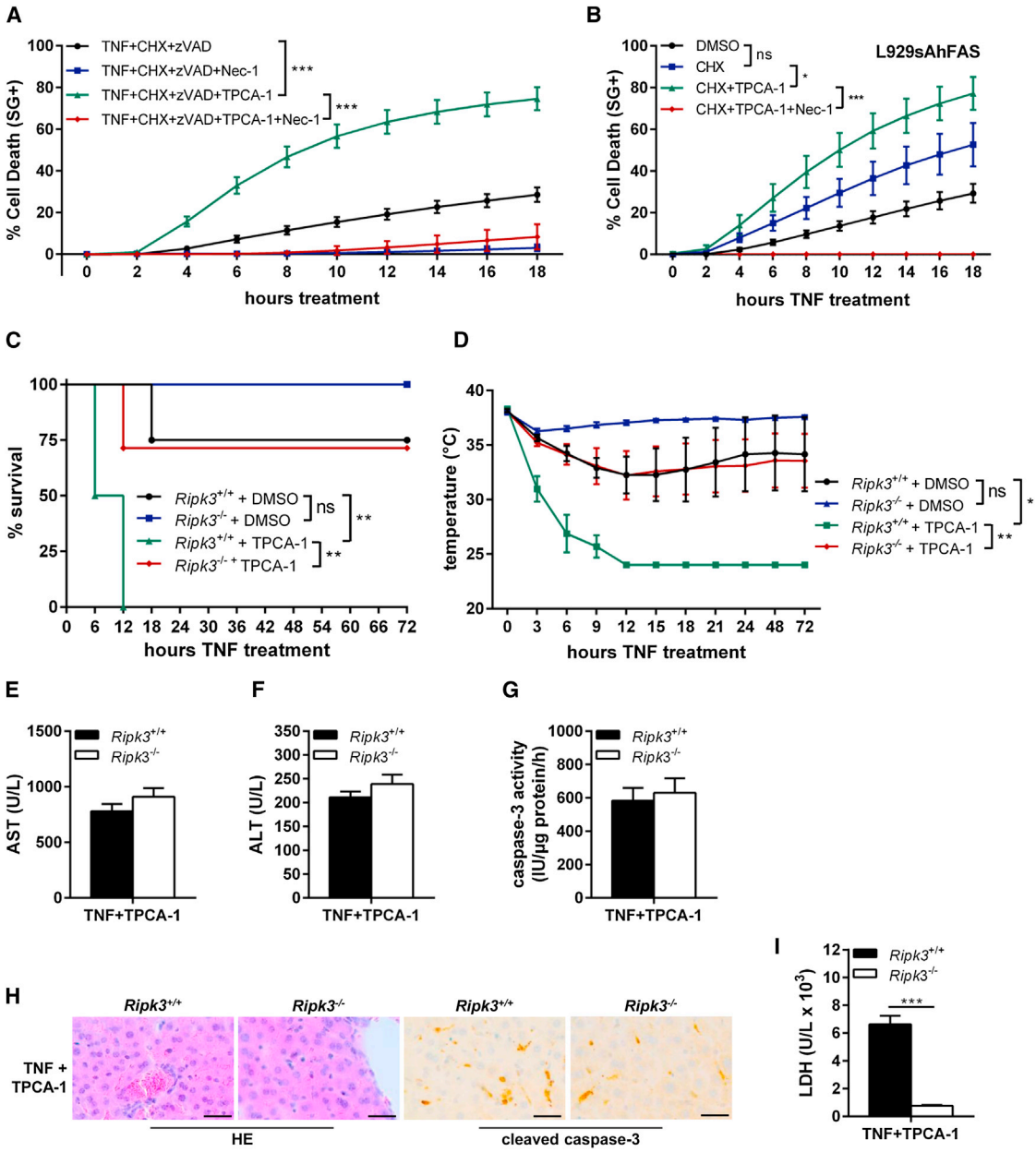

Figure 7. IKKα/IKKβ Protect Cells from RIPK1 Kinase-Dependent Necroptosis Independently of NF-κB

(A and B) *Ripk1*$^{+/+}$ MEFs (A) and L929sAhFas cells (B) were stimulated with hTNF (20 ng/ml in A and 33 pg/ml in B) in the presence of the indicated compounds, and cell death was measured as a function of time by SytoxGreen positivity.

(C) Cumulative survival rates of littermate *Ripk3*$^{+/+}$ and *Ripk3*$^{-/-}$ C57BL/6J females injected with TPCA-1 20 min prior to injection with mTNF (*Ripk3*$^{+/+}$ n = 4, and *Ripk3*$^{-/-}$ n = 7).

(D) Body temperature as a function of time.

(E, F, and I) Blood AST (E), ALT (F), and LDH (I) levels determined 3 hr post-TNF injection (*Ripk3*$^{+/+}$ n = 4, and *Ripk3*$^{-/-}$ n = 3).

(G and H) Caspase-3 activity in liver samples (*Ripk3*$^{+/+}$ n = 4, and *Ripk3*$^{-/-}$ n = 3) isolated 3 hr post-TNF injection and determined by Ac-DEVD-AMC fluorescence assay (G) or anti-cleaved caspase-3 staining (H).

Scale bar, 25 μm. For the in vitro cell death results, error bars represent the SEM of three independent experiments. For the in vivo results, error bars represent the SEM of the indicated n values.

Statistical Analysis

Statistical analysis was performed with GraphPad Prism V6 software (GraphPad). All cell death data are presented as mean ± SEM of three independent experiments. Cellular caspase-3 activation data are presented as mean ± SD of one representative experiment. Temperature data, serum AST levels, serum ALT levels, serum LDH levels, and liver caspase-3 activity are presented as mean ± SEM of the indicated n values. Statistical significance for cell death, AST, ALT, LDH, and caspase-3 activity was determined using two-way

ANOVA followed by a post hoc Bonferroni test to correct for multiple testing between the samples. Survival curves were compared using log-rank Mantel-Cox test. Significance between samples is indicated in the figures as follows: *p < 0.05; **p < 0.01; ***p < 0.001; and ns, non-significant.

SUPPLEMENTAL INFORMATION

Supplemental Information includes Supplemental Experimental Procedures and seven figures and can be found with this article online at http://dx.doi.org/10.1016/j.molcel.2015.07.032.

AUTHOR CONTRIBUTIONS

Y.D., S.J.-L., and M.J.M.B. designed experiments, performed experiments, and analyzed the results. T.D. and E.T. performed experiments. J.B. and P.J.G. generated essential tools for the study. P.G. and A.J.R.H. performed the mass spectrometry experiment and analyzed the obtained results. E.D. contributed to the design of experiments, generated tools, and contributed to the analysis of the results. P.V. contributed to the design of the experiments and the analysis of the results. Y.D. and M.J.M.B. wrote the manuscript.

ACKNOWLEDGMENTS

We are grateful to V. Dixit and K. Newton (Genentech, USA) for the *Ripk3* mice, D. Vucic (Genentech, USA) for compound BV6, J. Silke (Walter+Eliza Hall, Australia) for the *ciap1/2* MEFs and *Sharpin* MDFs, and S. Hofmans and K. Augustyns (University of Antwerp, Belgium) for the synthesis of Nec-1s. We thank W. Declercq, S. Lefebvre, N. Takahashi, and M. Aguileta for scientific discussion and J. Dekeyser, M. Sze, and Monica T. Fernandes for technical assistance. M.J.M.B. has a tenure track position within the Multidisciplinary Research Program of Ghent University (GROUP-ID). Y.D. is holder of an IWT doctoral fellowship. S.J.-L. is an omics@vib postdoctoral fellow (co-funded by Marie Curie COFUND initiative). Research in the Vandenabeele unit is supported by Belgian grants (IAP 7/32), Flemish grants (FWO G087511, G097311, G0A4512N, G078713N, G017212N, and G013715N; Methusalem BOF09/01M00709), Ghent University grants (MRP, GROUP-ID consortium), grants from the Foundation Against Cancer (F94 and 2010-162), and grants from the VIB. Y.D. and T.D. are now paid by the Methusalem grant. P.G. and A.J.R.H. are supported by the PRIME-XS project, grant number 262067, funded by the European Union 7th Framework Program, and the Netherlands Organization for Scientific Research (NWO) supported large-scale proteomics facility Proteins@Work (project 184.032.201) embedded in the Netherlands Proteomics Centre. Dejardin research group is supported by the Plan Cancer Action 29, IAP7/32 and Centre AntiCancéreux ULg. J.B. and P.J.G. are employees of GlaxoSmithKline.

Received: November 26, 2014
Revised: June 15, 2015
Accepted: July 30, 2015
Published: September 3, 2015

REFERENCES

Baldwin, A.S. (2012). Regulation of cell death and autophagy by IKK and NF-κB: critical mechanisms in immune function and cancer. Immunol. Rev. *246*, 327–345.

Baud, V., and Karin, M. (2009). Is NF-kappaB a good target for cancer therapy? Hopes and pitfalls. Nat. Rev. Drug Discov. *8*, 33–40.

Beg, A.A., Sha, W.C., Bronson, R.T., Ghosh, S., and Baltimore, D. (1995). Embryonic lethality and liver degeneration in mice lacking the RelA component of NF-kappa B. Nature *376*, 167–170.

Berger, S.B., Kasparcova, V., Hoffman, S., Swift, B., Dare, L., Schaeffer, M., Capriotti, C., Cook, M., Finger, J., Hughes-Earle, A., et al. (2014). Cutting Edge: RIP1 kinase activity is dispensable for normal development but is a key regulator of inflammation in SHARPIN-deficient mice. J. Immunol. *192*, 5476–5480.

Bertrand, M.J., Milutinovic, S., Dickson, K.M., Ho, W.C., Boudreault, A., Durkin, J., Gillard, J.W., Jaquith, J.B., Morris, S.J., and Barker, P.A. (2008). cIAP1 and cIAP2 facilitate cancer cell survival by functioning as E3 ligases that promote RIP1 ubiquitination. Mol. Cell *30*, 689–700.

Cho, Y.S., Challa, S., Moquin, D., Genga, R., Ray, T.D., Guildford, M., and Chan, F.K. (2009). Phosphorylation-driven assembly of the RIP1-RIP3 complex regulates programmed necrosis and virus-induced inflammation. Cell *137*, 1112–1123.

Conte, M.I., Pescatore, A., Paciolla, M., Esposito, E., Miano, M.G., Lioi, M.B., McAleer, M.A., Giardino, G., Pignata, C., Irvine, A.D., et al. (2014). Insight into IKBKG/NEMO locus: report of new mutations and complex genomic rearrangements leading to incontinentia pigmenti disease. Hum. Mutat. *35*, 165–177.

Decker, K., and Keppler, D. (1974). Galactosamine hepatitis: key role of the nucleotide deficiency period in the pathogenesis of cell injury and cell death. Rev. Physiol. Biochem. Pharmacol. *71*, 77–106.

Degterev, A., Maki, J.L., and Yuan, J. (2013). Activity and specificity of necrostatin-1, small-molecule inhibitor of RIP1 kinase. Cell Death Differ. *20*, 366.

Dejardin, E., Droin, N.M., Delhase, M., Haas, E., Cao, Y., Makris, C., Li, Z.W., Karin, M., Ware, C.F., and Green, D.R. (2002). The lymphotoxin-beta receptor induces different patterns of gene expression via two NF-kappaB pathways. Immunity *17*, 525–535.

Dondelinger, Y., Aguileta, M.A., Goossens, V., Dubuisson, C., Grootjans, S., Dejardin, E., Vandenabeele, P., and Bertrand, M.J. (2013). RIPK3 contributes to TNFR1-mediated RIPK1 kinase-dependent apoptosis in conditions of cIAP1/2 depletion or TAK1 kinase inhibition. Cell Death Differ. *20*, 1381–1392.

Ea, C.K., Deng, L., Xia, Z.P., Pineda, G., and Chen, Z.J. (2006). Activation of IKK by TNFalpha requires site-specific ubiquitination of RIP1 and polyubiquitin binding by NEMO. Mol. Cell *22*, 245–257.

Gentle, I.E., Wong, W.W., Evans, J.M., Bankovacki, A., Cook, W.D., Khan, N.R., Nachbur, U., Rickard, J., Anderton, H., Moulin, M., et al. (2011). In TNF-stimulated cells, RIPK1 promotes cell survival by stabilizing TRAF2 and cIAP1, which limits induction of non-canonical NF-kappaB and activation of caspase-8. J. Biol. Chem. *286*, 13282–13291.

Gerlach, B., Cordier, S.M., Schmukle, A.C., Emmerich, C.H., Rieser, E., Haas, T.L., Webb, A.I., Rickard, J.A., Anderton, H., Wong, W.W., et al. (2011). Linear ubiquitination prevents inflammation and regulates immune signalling. Nature *471*, 591–596.

Haas, T.L., Emmerich, C.H., Gerlach, B., Schmukle, A.C., Cordier, S.M., Rieser, E., Feltham, R., Vince, J., Warnken, U., Wenger, T., et al. (2009). Recruitment of the linear ubiquitin chain assembly complex stabilizes the TNF-R1 signaling complex and is required for TNF-mediated gene induction. Mol. Cell *36*, 831–844.

Hayden, M.S., and Ghosh, S. (2012). NF-κB, the first quarter-century: remarkable progress and outstanding questions. Genes Dev. *26*, 203–234.

Hayden, M.S., and Ghosh, S. (2014). Regulation of NF-κB by TNF family cytokines. Semin. Immunol. *26*, 253–266.

He, S., Wang, L., Miao, L., Wang, T., Du, F., Zhao, L., and Wang, X. (2009). Receptor interacting protein kinase-3 determines cellular necrotic response to TNF-alpha. Cell *137*, 1100–1111.

Hinz, M., and Scheidereit, C. (2014). The IκB kinase complex in NF-κB regulation and beyond. EMBO Rep. *15*, 46–61.

Hu, Y., Baud, V., Delhase, M., Zhang, P., Deerinck, T., Ellisman, M., Johnson, R., and Karin, M. (1999). Abnormal morphogenesis but intact IKK activation in mice lacking the IKKalpha subunit of IkappaB kinase. Science *284*, 316–320.

Irmler, M., Thome, M., Hahne, M., Schneider, P., Hofmann, K., Steiner, V., Bodmer, J.L., Schröter, M., Burns, K., Mattmann, C., et al. (1997). Inhibition of death receptor signals by cellular FLIP. Nature *388*, 190–195.

Kanayama, A., Seth, R.B., Sun, L., Ea, C.K., Hong, M., Shaito, A., Chiu, Y.H., Deng, L., and Chen, Z.J. (2004). TAB2 and TAB3 activate the NF-kappaB pathway through binding to polyubiquitin chains. Mol. Cell *15*, 535–548.

Karin, M., and Lin, A. (2002). NF-kappaB at the crossroads of life and death. Nat. Immunol. *3*, 221–227.

Kreuz, S., Siegmund, D., Scheurich, P., and Wajant, H. (2001). NF-kappaB inducers upregulate cFLIP, a cycloheximide-sensitive inhibitor of death receptor signaling. Mol. Cell. Biol. *21*, 3964–3973.

Kumari, S., Redouane, Y., Lopez-Mosqueda, J., Shiraishi, R., Romanowska, M., Lutzmayer, S., Kuiper, J., Martinez, C., Dikic, I., Pasparakis, M., and Ikeda, F. (2014). Sharpin prevents skin inflammation by inhibiting TNFR1-induced keratinocyte apoptosis. eLife, *3*, e03422.

Legarda-Addison, D., Hase, H., O'Donnell, M.A., and Ting, A.T. (2009). NEMO/IKKgamma regulates an early NF-kappaB-independent cell-death checkpoint during TNF signaling. Cell Death Differ. *16*, 1279–1288.

Li, Q., Van Antwerp, D., Mercurio, F., Lee, K.F., and Verma, I.M. (1999). Severe liver degeneration in mice lacking the IkappaB kinase 2 gene. Science *284*, 321–325.

Li, Q., Estepa, G., Memet, S., Israel, A., and Verma, I.M. (2000). Complete lack of NF-kappaB activity in IKK1 and IKK2 double-deficient mice: additional defect in neurulation. Genes Dev. *14*, 1729–1733.

Li, H., Kobayashi, M., Blonska, M., You, Y., and Lin, X. (2006). Ubiquitination of RIP is required for tumor necrosis factor alpha-induced NF-kappaB activation. J. Biol. Chem. *281*, 13636–13643.

Liu, Z.G., Hsu, H., Goeddel, D.V., and Karin, M. (1996). Dissection of TNF receptor 1 effector functions: JNK activation is not linked to apoptosis while NF-kappaB activation prevents cell death. Cell *87*, 565–576.

Liu, F., Xia, Y., Parker, A.S., and Verma, I.M. (2012). IKK biology. Immunol. Rev. *246*, 239–253.

Luedde, T., Beraza, N., Kotsikoris, V., van Loo, G., Nenci, A., De Vos, R., Roskams, T., Trautwein, C., and Pasparakis, M. (2007). Deletion of NEMO/IKKgamma in liver parenchymal cells causes steatohepatitis and hepatocellular carcinoma. Cancer Cell *11*, 119–132.

Mahoney, D.J., Cheung, H.H., Mrad, R.L., Plenchette, S., Simard, C., Enwere, E., Arora, V., Mak, T.W., Lacasse, E.C., Waring, J., and Korneluk, R.G. (2008). Both cIAP1 and cIAP2 regulate TNFalpha-mediated NF-kappaB activation. Proc. Natl. Acad. Sci. USA *105*, 11778–11783.

McQuade, T., Cho, Y., and Chan, F.K. (2013). Positive and negative phosphorylation regulates RIP1- and RIP3-induced programmed necrosis. Biochem. J. *456*, 409–415.

Micheau, O., and Tschopp, J. (2003). Induction of TNF receptor I-mediated apoptosis via two sequential signaling complexes. Cell *114*, 181–190.

Micheau, O., Lens, S., Gaide, O., Alevizopoulos, K., and Tschopp, J. (2001). NF-kappaB signals induce the expression of c-FLIP. Mol. Cell. Biol. *21*, 5299–5305.

Moulin, M., Anderton, H., Voss, A.K., Thomas, T., Wong, W.W., Bankovacki, A., Feltham, R., Chau, D., Cook, W.D., Silke, J., and Vaux, D.L. (2012). IAPs limit activation of RIP kinases by TNF receptor 1 during development. EMBO J. *31*, 1679–1691.

O'Donnell, M.A., and Ting, A.T. (2011). RIP1 comes back to life as a cell death regulator in TNFR1 signaling. FEBS J. *278*, 877–887.

O'Donnell, M.A., Legarda-Addison, D., Skountzos, P., Yeh, W.C., and Ting, A.T. (2007). Ubiquitination of RIP1 regulates an NF-kappaB-independent cell-death switch in TNF signaling. Curr. Biol. *17*, 418–424.

O'Donnell, M.A., Hase, H., Legarda, D., and Ting, A.T. (2012). NEMO inhibits programmed necrosis in an NFκB-independent manner by restraining RIP1. PLoS ONE *7*, e41238.

Panayotova-Dimitrova, D., Feoktistova, M., Ploesser, M., Kellert, B., Hupe, M., Horn, S., Makarov, R., Jensen, F., Porubsky, S., Schmieder, A., et al. (2013). cFLIP regulates skin homeostasis and protects against TNF-induced keratinocyte apoptosis. Cell Rep. *5*, 397–408.

Pasparakis, M., and Vandenabeele, P. (2015). Necroptosis and its role in inflammation. Nature *517*, 311–320.

Petersen, S.L., Wang, L., Yalcin-Chin, A., Li, L., Peyton, M., Minna, J., Harran, P., and Wang, X. (2007). Autocrine TNFalpha signaling renders human cancer cells susceptible to Smac-mimetic-induced apoptosis. Cancer Cell *12*, 445–456.

Podolin, P.L., Callahan, J.F., Bolognese, B.J., Li, Y.H., Carlson, K., Davis, T.G., Mellor, G.W., Evans, C., and Roshak, A.K. (2005). Attenuation of murine collagen-induced arthritis by a novel, potent, selective small molecule inhibitor of IkappaB Kinase 2, TPCA-1 (2-[(aminocarbonyl)amino]-5-(4-fluorophenyl)-3-thiophenecarboxamide), occurs via reduction of proinflammatory cytokines and antigen-induced T cell Proliferation. J. Pharmacol. Exp. Ther. *312*, 373–381.

Rickard, J.A., Anderton, H., Etemadi, N., Nachbur, U., Darding, M., Peltzer, N., Lalaoui, N., Lawlor, K.E., Vanyai, H., Hall, C., et al. (2014). TNFR1-dependent cell death drives inflammation in Sharpin-deficient mice. eLife *3*, e03464.

Rudolph, D., Yeh, W.C., Wakeham, A., Rudolph, B., Nallainathan, D., Potter, J., Elia, A.J., and Mak, T.W. (2000). Severe liver degeneration and lack of NF-kappaB activation in NEMO/IKKgamma-deficient mice. Genes Dev. *14*, 854–862.

Sun, L., Wang, H., Wang, Z., He, S., Chen, S., Liao, D., Wang, L., Yan, J., Liu, W., Lei, X., and Wang, X. (2012). Mixed lineage kinase domain-like protein mediates necrosis signaling downstream of RIP3 kinase. Cell *148*, 213–227.

Takeda, K., Takeuchi, O., Tsujimura, T., Itami, S., Adachi, O., Kawai, T., Sanjo, H., Yoshikawa, K., Terada, N., and Akira, S. (1999). Limb and skin abnormalities in mice lacking IKKalpha. Science *284*, 313–316.

Van Antwerp, D.J., Martin, S.J., Kafri, T., Green, D.R., and Verma, I.M. (1996). Suppression of TNF-alpha-induced apoptosis by NF-kappaB. Science *274*, 787–789.

Vanlangenakker, N., Vanden Berghe, T., Bogaert, P., Laukens, B., Zobel, K., Deshayes, K., Vucic, D., Fulda, S., Vandenabeele, P., and Bertrand, M.J. (2011). cIAP1 and TAK1 protect cells from TNF-induced necrosis by preventing RIP1/RIP3-dependent reactive oxygen species production. Cell Death Differ. *18*, 656–665.

Walczak, H. (2011). TNF and ubiquitin at the crossroads of gene activation, cell death, inflammation, and cancer. Immunol. Rev. *244*, 9–28.

Wang, C.Y., Mayo, M.W., Korneluk, R.G., Goeddel, D.V., and Baldwin, A.S., Jr. (1998). NF-kappaB antiapoptosis: induction of TRAF1 and TRAF2 and c-IAP1 and c-IAP2 to suppress caspase-8 activation. Science *281*, 1680–1683.

Wang, L., Du, F., and Wang, X. (2008). TNF-alpha induces two distinct caspase-8 activation pathways. Cell *133*, 693–703.

Wilson, N.S., Dixit, V., and Ashkenazi, A. (2009). Death receptor signal transducers: nodes of coordination in immune signaling networks. Nat. Immunol. *10*, 348–355.

Wu, C.J., Conze, D.B., Li, T., Srinivasula, S.M., and Ashwell, J.D. (2006). Sensing of Lys 63-linked polyubiquitination by NEMO is a key event in NF-kappaB activation [corrected]. Nat. Cell Biol. *8*, 398–406.

Zhang, D.W., Shao, J., Lin, J., Zhang, N., Lu, B.J., Lin, S.C., Dong, M.Q., and Han, J. (2009). RIP3, an energy metabolism regulator that switches TNF-induced cell death from apoptosis to necrosis. Science *325*, 332–336.

Zhao, J., Jitkaew, S., Cai, Z., Choksi, S., Li, Q., Luo, J., and Liu, Z.G. (2012). Mixed lineage kinase domain-like is a key receptor interacting protein 3 downstream component of TNF-induced necrosis. Proc. Natl. Acad. Sci. USA *109*, 5322–5327.